

The Role of Al Reaction Rate in the Damage Effect and Energy Output of RDX-Based Aluminized Explosives in Concrete

Zhengqing Zhou,^[a] Jianguo Chen,*^[a] Hongyong Yuan,^[a] and Jianxin Nie^[b]

Abstract: This paper aims to improve the understanding of how the aluminum reaction rate affects the damage effect and energy output of RDX-based aluminized explosives in concrete. A calculation method for the dynamic response of concrete and energy output of RDX-based aluminized explosive is proposed based on the time-dependent Jones-Wilkins-Lee equation of state (JWL-EOS), cavity expansion model and energy partition theory, which is in turn verified through experiments with 70 g RDX/Al/wax (65%/30%/5%) charge embedded in concrete. Based on the proposed method, the dynamic response of concrete and energy output of RDX/Al/wax with four different aluminum reaction

rates were calculated. The results indicate a positive correlation between the crushed region radius and the aluminum reaction rate, and that the cracked region radius is inversely proportional to the aluminum reaction rate. For the energy output of RDX/Al/wax, the shock wave energy grows with increasing aluminum reaction rate, while the detonation products expansion energy increases and then drops with rising aluminum reaction rate, peaking at 2.37 MJ/kg when the Al reaction rate constant $M=0.02$. The calculation method presented in this paper are of great significance for investigating and improving the performance of RDX-based aluminized explosives in concrete.

Keywords: Aluminized explosives · Aluminum reaction rate · Energy output · Damage effect

1 Introduction

Aluminum powder is often added to explosives to improve performance [1–5] as it increases the detonation heat, the pressure impulse in air experiments, and the bubble energies in underwater experiments. And the aluminum reaction rate is mainly determined by the aluminum particle size when the formula of aluminized explosive is certain [6–7].

Depending on the aluminum reaction rate during the explosion of aluminized explosives, aluminum reaction can occur in three phases [2,8,9]. Phase I is the reaction in the detonation reaction zone (approximately less than 200 ns), Phase II is the reaction in the post-detonation early expansion phase (4–10 μ s), and Phase III is the late reaction that contributes to blast effects (1–100 ms). Therefore, aluminum reaction rate has an important influence on the performance of aluminized explosives. Regarding explosives in the air, Brousseau et al. [10] measured the shock wave pressure and impulse for Comp. B/Al (10% Al) with different aluminum particle sizes, and the experimental results show that there is no noticeable difference in performance among different aluminum types in Comp. B/Al. Lefrancois and Gallic [11] obtained a similar conclusion, the conclusion shows that Alex (100–200 nm) and 5 μ m aluminum gave the same performance in air-blast tests of cylindrical charges. In the water, Miller and Guirguis [12] calculated energy output of aluminized explosive by using DYNA2D hydro-

code in which a time-dependent JWL-EOS was introduced in order to account for the aluminum reaction rate, the calculation showed that the slower aluminum reaction rate, the higher the bubble energy. Concrete is one of the most widely used materials in military facilities. In the concrete, Pei et al. [13] performed explosion experiments with 70 g RDX-based aluminized explosive, the experimental results show that the damage area of RDX/Al/wax (80%/15%/5%) is 10% larger than pure RDX. Zhou et al. [14] measured the shock wave pressures in the affected concrete bodies by using manganin pressure sensor, the results indicated that the pressure impulse of RDX/Al/wax (80%/15%/5%) is 42% higher than pure RDX. Aluminized explosives perform well in the concrete, but the role of aluminum reaction in the performance of RDX-based aluminized explosives in concrete has rarely been investigated.

[a] Z. Zhou, J. Chen, H. Yuan
*Institute of Public Safety Research
Department of Engineering Physics
Tsinghua University
Haidian District, Beijing, 100084, P.R.China*
**e-mail: chenjianguo@mail.tsinghua.edu.cn
zhouzheng_qing@163.com*

[b] J. Nie
*State Key Laboratory of Explosion Science and Technology
Beijing Institute of Technology
Haidian District, Beijing, 100081, P.R.China*

At present, RDX-based aluminized explosive is one of the most widely used aluminized explosives. Therefore, RDX-based aluminized explosives were chosen as the research object of this study. In this study, the calculation method for the damage effect and energy output of RDX-based aluminized explosive is presented. In addition, experiments with 70 g cylindrical aluminized explosive charge embedded in concrete were performed to verify the calculation method. And then, the effects of the aluminum reaction rate on the damage effect and energy output of aluminized explosive were studied.

2 Calculation Method for the Damage Effect and Energy Output of RDX-based Aluminized Explosive in Concrete

The damage effect of RDX-based aluminized explosives in concrete can be evaluated by the dynamic response of concrete. However, it is difficult to obtain the dynamic response process of concrete under blast loading due to limitations of experimental techniques. Moreover, aluminized explosive experiment in concrete has high cost and long cycle. Using cavity expansion model to study the concrete damage not only helps understand the specific damage process, but also reduces the experimental cost.

According to the time-dependent JWL-EOS, cavity expansion model and energy partition theory, the dynamic response of concrete and energy output of aluminized explosive can be calculated, and the calculation method is shown in Figure 1.

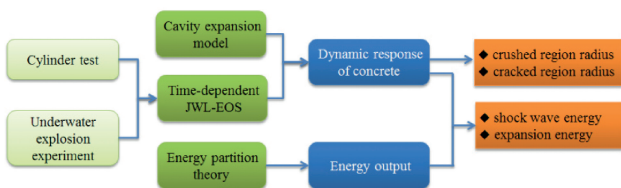


Figure 1. Calculation method for the damage effect and energy output of aluminized explosives.

2.1 Time-dependent JWL Equation of State

The cylinder tests and the underwater explosion experiments were performed to obtain the time-dependent JWL-EOS parameters of aluminized explosives. The explosives used in this study are comprised of RDX (65 wt.%), aluminum powder (30 wt.%), and wax (5 wt.%). Aluminum powder, with particle sizes of 10 μm and 2 μm , were added to the explosives at a mass ratio of 2:1. In aluminized explosives, a substantial amount of energy is released after the C-J surface. In order to account for the late energy re-

lease in aluminized explosive, the time-dependent JWL-EOS has been used to describe the relationship between detonation product pressure P and relative volume V [12, 15, 16], the equation is:

$$P = A(1 - \omega/R_1 V) \exp(-R_1 V) + B(1 - \omega/R_2 V) \exp(-R_2 V) + \omega(E + \lambda Q)/V \quad (1)$$

Where A , B , R_1 , R_2 , ω (the Gruneisen coefficient) are constants; P is pressure; V is relative volume; E is the energy content of the explosive that sustains the detonation CJ conditions; Q is the energy release of aluminum reaction after the CJ plane; λ is reaction extent of aluminum. The general expression of aluminum reaction rate [15, 17, 18] is

$$d\lambda/dt = M(1 - \lambda)^a P^b \quad (2)$$

Where the reaction rate constant M is the parameter related to the particle size of aluminum powder, a higher M is associated with a faster aluminum reaction rate, moreover, aluminum reaction rate is inversely proportional to particle size of aluminum powder [19], therefore, M is also inversely proportional to the particle size of aluminum powder. a , b are the reaction rate exponents.

In RDX/Al/wax (65%/30%/5%), our previous work [20] has examined that Al requires 2–3 ms to react completely by the driven metal-rod test. However, the effective acting time in the Ø25 mm cylinder test is no more than 17 μs , during this time, the acceleration of wall has almost been completed. Thus, it is assumed that energy release of Al participate in reactions with detonation products do not accelerate wall in cylinder tests, i.e., the value of λ is equal to 0. So the Gruneisen coefficients can be obtained from the cylinder test in this paper. However, in the underwater explosion experiment, it has much longer characteristic times than cylinder test. Al have enough time to react with detonation products, so the reaction rate parameters M , a , b can be obtained by underwater explosion experiments.

According to the result of the wall radial velocity in cylinder tests and the shock wave pressure in underwater explosion experiments (Figure 2 and Figure 3), the time-dependent JWL-EOS parameters (Gruneisen coefficients, M , a , b) can be determined by iterating these variables in AUTO-DYN hydrocode simulations until the experimental values are reproduced. Figure 2 and Figure 3 show the calculated wall velocity and shock wave pressure are all in good agreement with the experimental data. The detailed description of this method has been provided in our previous work [21]. The obtained time-dependent JWL-EOS parameters of RDX/Al/wax (65%/30%/5%) are shown in Table 1.

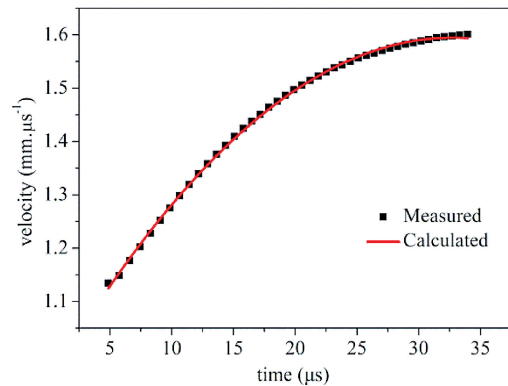
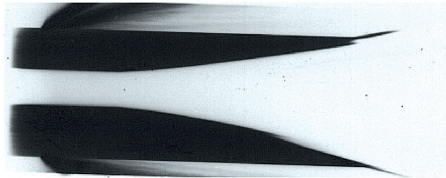


Figure 2. X-ray photograph of a copper tube driven by the detonation products (left), Comparison between the calculated and experimental results (right).

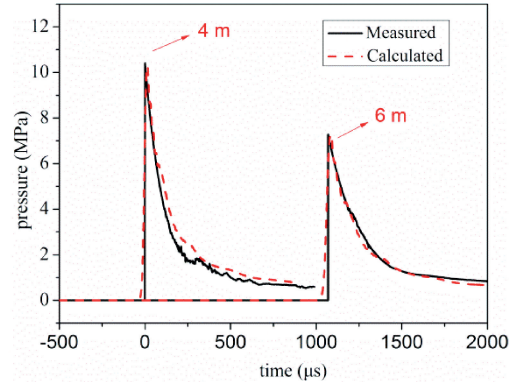
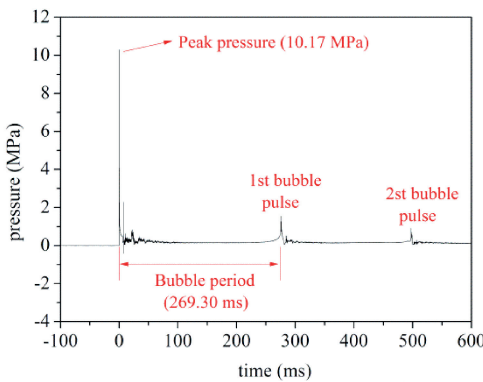


Figure 3. A typical pressure history measured at 4 m away from the charge (left), Comparison between the calculated and experimental results (right).

Table 1. Characteristics and JWLEOS parameters of RDX/Al/wax (65%/30%/5%).

Parameter	value	Parameter	value
Density (kg/m^3)	1870	R_1	5.94
Detonation velocity (m/s)	7879	R_2	1.78
Detonation pressure (GPa)	22.21	ω	0.38
A (GPa)	2225.00	M	0.0075
B (GPa)	21.59	a	0.40
C (GPa)	2.70	b	0.25

2.2 Cavity Expansion Model

The dynamic response of concrete under blast loading is described by the cavity expansion model [22–25]. According to the cavity expansion model, the response region in concrete consists of four distinct zones: cavity, crushed region, cracked region and elastic region. The dynamic behavior of concrete materials under blast loading is as follows

(1) Crushed Region Development

After the explosive detonation, the whole blasthole is filled with gaseous detonation products with very high pressure and temperature. Generating radial compressive stress is much higher than the strength of the concrete, so the crushed region appears. It is assumed that the speed of the crushed region boundary is higher than the dilatational elastic wave speed in the first stage. The schematic illustration of crushed region development is shown in Figure 4. The crushed region is bounded by x_1 and x_2 .

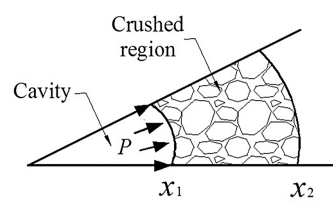


Figure 4. Schematic illustration of crushed region development.

(2) Crushed-elastic Region Development

As time increases, the speed of the crushed region boundary decreases. It is assumed that the speed of the crushed region boundary is equal to the elastic wave velocity when the dimensionless time is τ , and then the elastic region appears. The crushed and elastic regions develop at the same time, as shown in Figure 5.

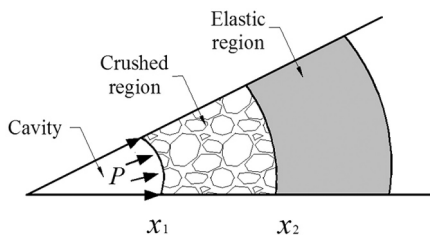


Figure 5. Crushed-elastic region in spherical cavity.

(3) Crushed-cracked-elastic Region Development

As time increases, the speed of the crushed region boundary will decrease further. The radial cracked region appears when the tensile hoop stress equals the tensile strength of the concrete. At this moment, the dynamic response regions entered the third stage (crushed-cracked-elastic region development), which is shown in Figure 6.

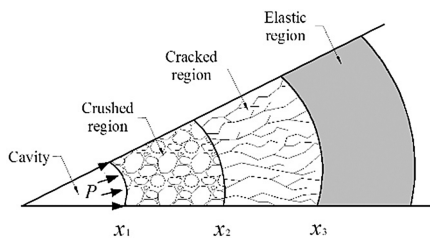


Figure 6. Crushed-cracked-elastic region in spherical cavity.

Therefore, if the JWL-EOS (i.e., the relationship between detonation product pressure P and relative volume V) of aluminized explosive is determined, the dynamic response process of concrete under blast loading can be calculated, and then the radii of the crushed and cracked regions (x_1 and x_2) can be obtained [26–27].

2.3 Energy Partition Theory

According to the energy partition theory [28], the explosive energy released in concrete can be divided into shock wave energy, detonation products expansion energy and other

energy, as shown in Figure 7. Point a represents the state when the cracks appear, and point b corresponds to the state with the stopping of crack growth. Based on the calculation results for the dynamic response process of concrete, the shock wave energy and the detonation products expansion energy can be calculated with the following equations

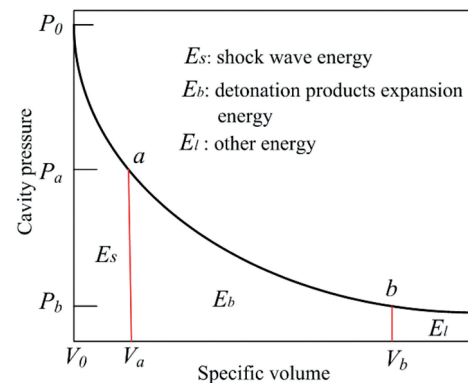


Figure 7. Schematic diagram of the energy partition in concrete.

$$E_s = \int_{V_0}^{V_a} P dV \quad (3)$$

$$E_b = \int_{V_a}^{V_b} P dV \quad (4)$$

Where P is detonation product pressure, $V=v/v_0$ is relative volume, v_0 is charge volume.

3 Aluminized Explosive Experiments in Concrete

In order to verify the calculation method described in Section 2, aluminized explosive experiments in concrete were performed. The experiments with 70 g cylindrical RDX/Al/

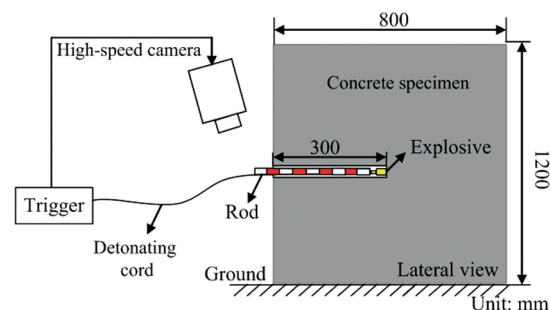


Figure 8. Schematic diagram of the experimental setup.

Table 2. Properties of the concrete.

Parameter	Value	Parameter	Value
Density (kg/m^3)	2300	Uniaxial compressive strength (MPa)	32.5
Young's modulus (GPa)	30.5	Tensile strength (MPa)	2.86
Poisson's ratio	0.25	Internal friction angle (deg)	43
Speed of sound (m/s)	3990	Cohesion (MPa)	4.9

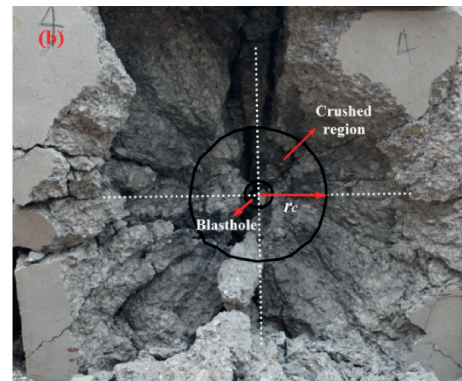
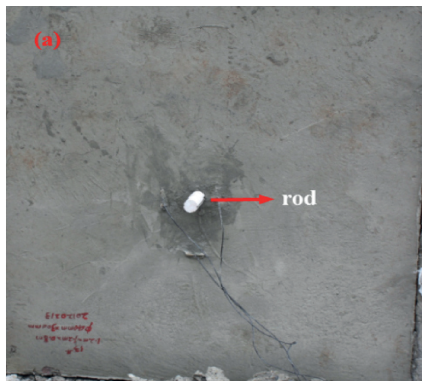
wax (65%/30%/5%) charge embedded in concrete were performed to verify the accuracy of the calculation results. Figure 8 shows a schematic diagram of experimental configuration. Each concrete specimen is a square plate ($1.2 \text{ m} \times 1.2 \text{ m} \times 0.8 \text{ m}$) with a cylindrical bore in the center of the specimen. Explosive charges were buried in concrete targets. The radius of the blasthole is 0.02 m. The concrete mixture used consists of cement, sand, crushed basalt and other components, as specified in Zhou et al. [14]. The physical properties of the concrete are listed in Table 2. The experiments for RDX-based aluminized explosives were performed in sextuplicate. A typical experimental result for concrete target is presented in Figure 9. As can be seen from Figure 9, the radii of the crushed and cracked regions

Table 3. Experimental data of crushed region radius and expansion energy.

Test no.	Crushed region radius r_c (m)	Average r_c (m)	Rod kinetic energy (MJ)	Detonation products expansion energy (MJ/kg)
1#	0.137	0.131	9.49	2.03
2#	0.123		9.18	1.94
3#	0.150		9.80	2.07
4#	0.131		10.05	2.12
5#	0.115		9.78	2.06
6#	0.130		9.80	2.07

can be measured according to the crack propagation path. In addition, the process of a rod exiting from the blasthole was captured by a high-speed camera, which is shown in Figure 10. According to the high-speed camera images, the kinetic energy of the rod was obtained using the image processing method [29], and then the detonation products expansion energy could be determined [30]. A summary of the experimental results is presented in Table 3.

In the meantime, the crushed region radius and detonation products expansion energy are calculated by the cavity expansion model and energy partition theory. The calculations are in reasonably good agreement with the ex-

**Figure 9.** Pretest (a) and posttest (b) photographs of concrete target.**Figure 10.** The process of a rod exiting from the blasthole.

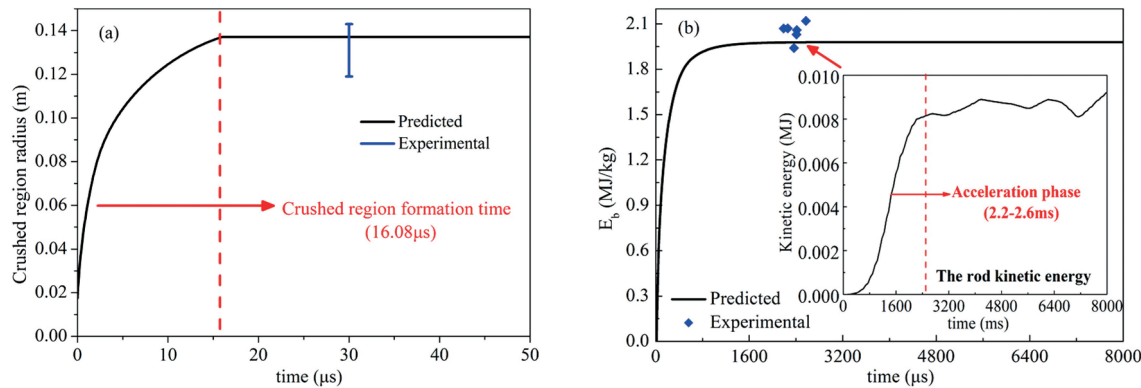


Figure 11. Comparison of the predicted results with the experimental data. (a) Crushed region radius. (b) Expansion energy.

perimental data, which is shown in Figure 11. This means that the calculation method and the time-dependent JLW-EOS parameters presented in this study is valid. Therefore, the dynamic response of concrete and the energy output of aluminized explosive can be predicted by this method.

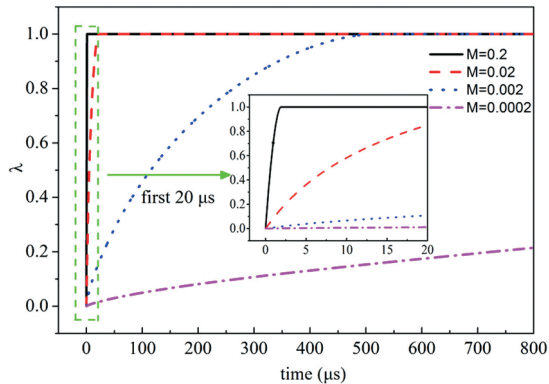


Figure 12. Time-dependence of aluminum reaction extent for different M .

4 Sensitivity Analysis for the Aluminum Reaction Rate

The aluminum reaction rate in RDX/Al/wax (65%/30%/5%) can be obtained by Eq. (2). In section 2.1, the parameters M , a , b in Eq. (2) have been determined by underwater explosion experiments, and the values of parameters M , a , and b are 0.0075, 0.40, and 0.25, respectively.

In order to more conveniently study the effects of the aluminum reaction rate on the damage effect and energy output of aluminized explosive, it is assumed that the parameters a and b are constant ($a=0.40$, $b=0.25$), and then the effects of aluminum reaction rates on the damage effect and energy output of aluminized explosive are studied by adjusting the value of parameter M . In this study, four different M (0.0002, 0.002, 0.02 and 0.2) are taken into account. The aluminum reaction extent versus time is given in Figure 12. The time required for complete reaction of aluminum ($\lambda=1$) is 7634.5 μs, 480.7 μs, 29.5 μs and 1.6 μs, respectively.

The radii of the crushed and cracked regions as functions of time are calculated by using the method presented in section 2, as shown in Figure 13. Figure 13 (a) shows that the crushed region radius grows with an increase in M from

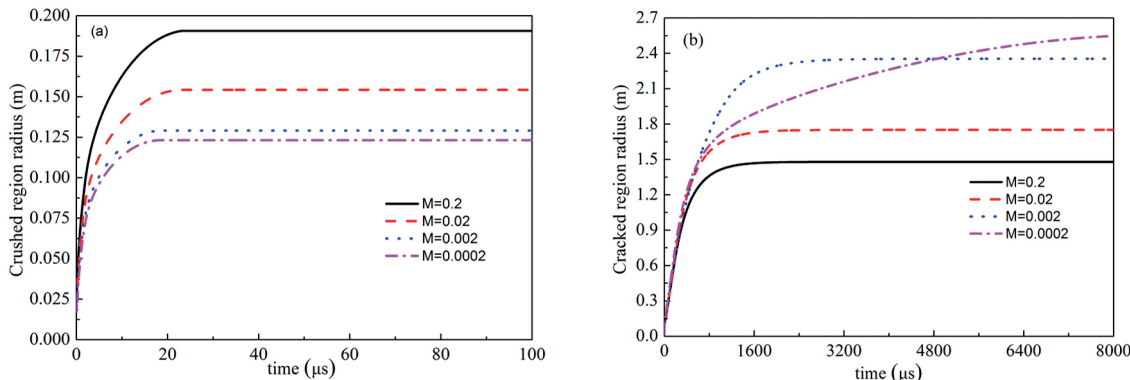


Figure 13. The development of the dynamic response regions. (a) Crushed region. (b) Cracked region.

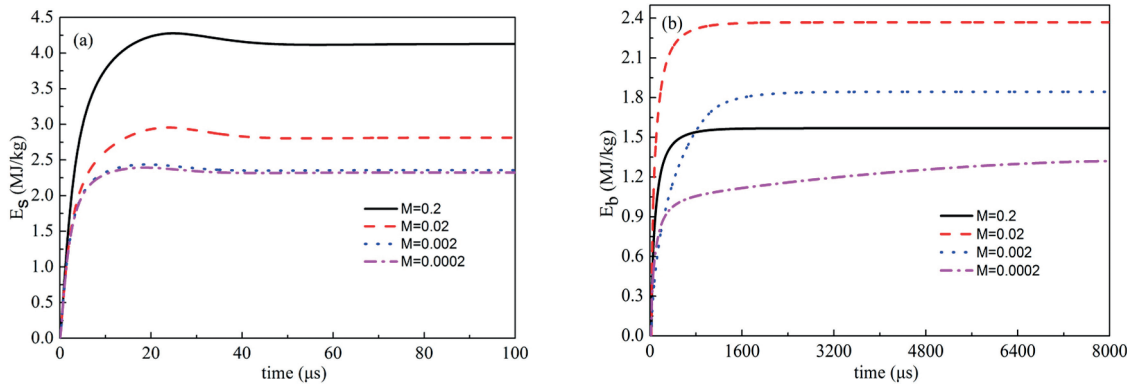


Figure 14. (a) Shock wave energy and (b) Detonation products expansion energy vs. time for different M .

0.0002 to 0.2, in other words, the crushed region radius increases with rising aluminum reaction rate. This is because the crushed region is formed within 20 μs after the detonation of explosive. During this time, the aluminum reaction extent is 0.011, 0.12, 0.81 and 1, respectively. A higher M is associated with a faster energy release of aluminum reaction, which leads to more energy to support the development of the crushed region. In Figure 13 (b), The cracked region radius for $M=0.0002$, 0.002, 0.02 and 0.2 is 2.54 m, 2.35 m, 1.76 m and 1.49 m, respectively. The cracked region radius is inversely proportional to aluminum reaction rate, which suggests that the slow energy release is conducive to the crack propagation. This is because the crack region formation time corresponding to four different aluminum reaction rates is 7890 μs , 3163 μs , 2307 μs , and 1849 μs , respectively. During this time, the aluminum powder for four different aluminum reaction rates has been completely reacted, which means that the total energy released by each kind of aluminum powder is the same. Therefore, the more energy that supports the development of the crushed region, the less energy will support the development of the crack region.

In addition, aluminum reaction rate plays an important role in the energy output of aluminized explosive. The shock wave energy and the detonation products expansion energy have been calculated with Eqs. (3) and (4). Figure 14 (a) shows the shock wave energy increases with increasing M , which indicates that the faster the aluminum reaction, the more shock wave energy converted from aluminum reaction. As observed in Figure 14 (b), the detonation products expansion energy increases as M increases from 0.0002 to 0.02, and then drops as M continues to grow from 0.02 to 0.2. The maximum detonation products expansion energy is 2.37 MJ/kg when $M=0.02$. Therefore, according to the research results, the energy output of aluminized explosives can be controlled by adjusting the aluminum reaction rate.

5 Conclusions

In this study, a calculation method for the damage effect and energy output of RDX-based aluminized explosives in concrete was proposed, and the calculation results are in reasonably good agreement with experimental data. Additionally, the influences of aluminum reaction rate on the damage effect and the energy output of aluminized explosive were studied, respectively. The main conclusions are as follows:

(1) The crushed region radius increases with an increase in M from 0.0002 to 0.2, i.e., the higher the aluminum reaction rate, the larger the crushed region radius. However, the cracked region radius is found to be inversely proportional to M , suggesting that the slow energy release is conducive to the crack propagation.

(2) An increase in aluminum reaction rate is associated with rise in shock wave energy. For the detonation products expansion energy, it first increases and then decreases with an increase in M from 0.0002 to 0.2, and the maximum detonation products expansion energy of 2.37 MJ/kg is reached when $M=0.02$.

The aluminum reaction rate is mainly determined by the aluminum particle size when the formula of aluminized explosive is certain, so the damage effect of aluminized explosives in concrete can be improved by adjusting the aluminum particle size. Further investigations should be performed on the specific relationship between aluminum particle size and aluminum reaction rate.

Acknowledgements

The authors are grateful for the support provided by the China Postdoctoral Science Foundation (Grant No. 2017M610091 and 2018T110106), National Natural Science Foundation of China (Grant No. 11802160) and The National Key Research and Development Program of China (Grant No. 2018YF0808606 and 2015BAK10B06).

References

- [1] K. P. Ruggirello, P. E. DesJardin, M. R. Baer, M. J. Kaneshige, E. S. Hertel, A Reaction Progress Variable Modeling Approach for Non-ideal Multiphase Explosives, *Int. J. Multiphase Flow* **2012**, *42*, 128–151.
- [2] J. M. Peuker, H. Krier, N. Glumac, Particle Size and Gas Environment Effects on Blast and Overpressure Enhancement in Aluminized Explosives, *Proc. Combust. Inst.* **2013**, *34*, 2205–2212.
- [3] T. Keicher, A. Happ, A. Kretschmer, U. Sirringhaus, R. Wild, Influence of Al/ammonium Perchlorate on the Performance of Underwater Explosives, *Propellants Explos. Pyrotech.* **1999**, *24*, 140–143.
- [4] V. W. Manner, S. J. Pemberton, J. A. Gunderson, T. J. Herrera, J. M. Lloyd, P. J. Salazar, P. Rae, B. C. Tappan, The Role of Aluminum in the Detonation and Post-detonation Expansion of Selected Cast HMX-Based Explosives, *Propellants Explos. Pyrotech.* **2012**, *37*, 198–206.
- [5] M. M. Swisdak, Explosion Effects and Properties Part II. Explosion Effect in Water, Report No. NSWC/WOL TR-76-116, Naval Surface Weapons Center White Oak Lab Silver Spring Md, **1978**.
- [6] M. W. Beckstead, Correlating Aluminum Burning Times, *Combust. Explos. Shock Waves* **2005**, *41*, 533–546.
- [7] B. T. Bojko, P. E. DesJardin, E. B. Washburn, On Modeling the Diffusion to Kinetically Controlled Burning Llimits of Micron-sized Aluminum Particles, *Combust. Flame* **2014**, *161*, 3211–3221.
- [8] W. A. Trzciński, L. Maiz, Thermobaric and Enhanced Blast Explosives-properties and Testing Methods, *Propellants Explos. Pyrotech.* **2015**, *40*, 632–644.
- [9] B. C. Tappan, V. W. Manner, J. M. Lloyd, S. J. Pemberton, Fast Reactions of Aluminum and Explosive Decomposition Products in a Post-detonation Environment, *AIP Conference Proceedings*. AIP (Chicago, USA, 26 June–1 July 2011). **2012**, *1426*, 271–274.
- [10] P. Brousseau, H. E. Dorsett, M. D. Cliff, C. J. Anderson, Detonation Properties of Explosives Containing Nanometric Aluminum Powder, *Proceedings of the 12th international detonation symposium*, (San Diego, USA, 26–11 August–16 August 2002) **2002**, 11–21.
- [11] A. Lefrancois, L. C. Gallic, Expertise of Nanometric Aluminium Powder on the Detonation Efficiency of Explosives. *Energetic materials-Ignition, combustion and detonation*, Karlsruhe, Germany, **2001**, 36–41.
- [12] P. J. Miller, R. H. Guirguis, Effects of Late Chemical Reactions of the Energy Partition in Non-ideal Underwater Explosions. In *High-pressure science and technology – 1993*. AIP Publishing **1994**, *309*, 1417–1420.
- [13] H. B. Pei, J. X. Nie, J. F. Qin, Z. Q. Zhou, Damage Effects of Explosion of RDX-Based Aluminized Explosives in Concrete, *Chin. J. High Press. Phys.* **2015**, *29*, 23–28.
- [14] Z. Q. Zhou, J. X. Nie, Z. C. Ou, J. F. Qin, Q. J. Jiao, Effects of the Aluminum Content on the Shock Wave Pressure and the Acceleration Ability of RDX-based Aluminized Explosives, *J. Appl. Phys.* **2014**, *116*, 144906.
- [15] P. J. Miller, A Reactive Flow Model with Coupled Reaction Kinetics for Detonation and Combustion in Non-ideal Explosives, In *MRS Proceedings*. Cambridge University Press, **1995**, pp. 413–20.
- [16] J. Lee, J. H. Kuk, Y. S. Cho, S. Y. Song, J. W. Lee, Numerical Modeling of Underwater Explosion Properties for an Aluminized Explosive, *Propellants Explos. Pyrotech.* **1997**, *22*, 337–346.
- [17] R. Wedberg, Using Underwater Explosion and Cylinder Expansion Tests to Calibrate Afterburn Models for Aluminized Explosives. *AIP Conference Proceedings*. AIP Publishing, **2018**, *1979*, pp. 1–7.
- [18] J. Z. Yue, Z. P. Duan, Z. Y. Zhang, Z. C. Ou, Research on Equation of State For Detonation Products of Aluminized Explosive. *J. Energ. Mater.* **2017**, pp. 481–89.
- [19] Z. Z. Zhou, J. G. Chen, H. Y. Yuan, J. X. Nie, Effects of Aluminum Particle Size on the Detonation Pressure of TNT/Al, *Propellants Explos. Pyrotech.* **2017**, pp. 1401–09.
- [20] Z. Q. Zhou, J. X. Nie, L. Zeng, Z. X. Jin, Q. J. Jiao, Effects of Aluminum Content on TNT Detonation and Aluminum Combustion using Electrical Conductivity Measurements, *Propellants Explos. Pyrotech.* **2016**, *41*, 84–91.
- [21] Z. Q. Zhou, J. X. Nie, X. Y. Guo, Q. J. Jiao, A New Method for Determining the Equation of State of Aluminized Explosive, *Chin. Phys. Lett.* **2015**, *32*, 016401.
- [22] M. J. Forrestal, D. Y. Tzou, A Spherical Cavity-expansion Penetration Model for Concrete Targets, *Int. J. Solids Struct.* **1997**, *34*, 4127–4146.
- [23] E. N. Sher, Taking into Account the Dynamics in Description of Fracture of Brittle Media by an Explosion of a Cord Charge, *J. Appl. Mech. Tech. Phys.* **1997**, *38*, 484–492.
- [24] E. N. Sher, N. I. Aleksandrova, Dynamics of Microfailures in Elastic Zone during Explosion of Spherical Charge in Rock, *J. Min. Sci.* **2001**, *37*, 475–481.
- [25] E. N. Sher, N. I. Aleksandrova, Effect of Borehole Charge Structure on the Parameters of a Failure Zone in Rocks under Blasting, *J. Min. Sci.* **2007**, *43*, 409–417.
- [26] S. Satapathy, Dynamic Spherical Cavity Expansion in Brittle Ceramics, *Int. J. Solids Struct.* **2001**, *38*, 5833–5845.
- [27] S. S. Satapathy, S. J. Bless, Cavity Expansion Resistance of Brittle Materials Obeying a Two-curve Pressure-shear Behavior, *J. Appl. Phys.* **2000**, *88*, 4004–4012.
- [28] M. R. Saharan, H. S. Mitri, Rock Fracturing by Explosive Energy Review of State-of-the-art, *Fragblast*, **2006**, *10*, 61–81.
- [29] Z. F. Sun, Q. Z. Li, X. L. Sun, J. H. Wu, T. G. Tang, Study on Standard Cylinder Test Technology and Data Processing Method. *Chin. J. High Press. Phys.* **2008**, *22*, 160–166.
- [30] J. A. Sanchidrian, P. Segarra, L. M. Lopez, Energy Components in Rock Blasting, *Int. J. Rock Mech. Min.* **2007**, *44*, 130–47.

Manuscript received: March 26, 2018

Revised manuscript received: September 2, 2018

Version of record online: January 11, 2019